Quark-Hadron Duality in DIS Form Factors and Drell-Yan Antiquark Flavor Asymmetries

Peter Ehlers

University of Minnesota, Morris
University of Washington

Mentor: Wally Melnitchouk

Table of Contents

Motivation for investigating Quark-Hadron duality

- Quark-Hadron duality tells us about the transition from hadronic degrees of freedom at low energies to quark and gluon degrees of freedom at high energies.

Motivation for investigating Quark-Hadron duality

- Quark-Hadron duality tells us about the transition from hadronic degrees of freedom at low energies to quark and gluon degrees of freedom at high energies.
- There has been considerable interest in quark-hadron duality at JLab.

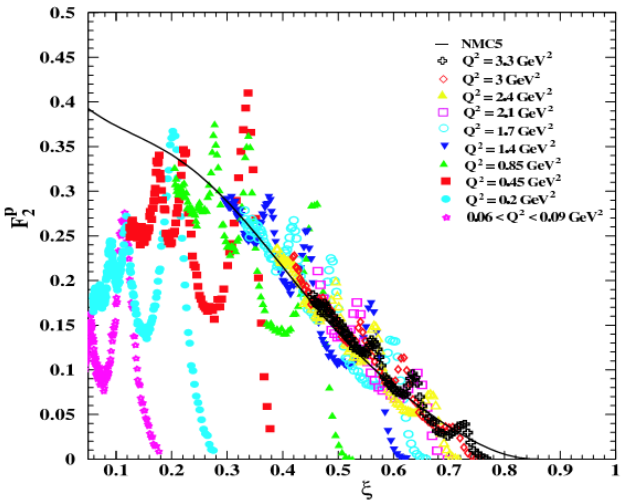

FIG. 12. Proton $\nu W_2^p = F_2^p$ structure function data from SLAC and Jefferson Lab in the resonance region in the range $0.06 < Q^2 < 3.30$ GeV^2, as indicated. The solid curve is a fit to deep inelastic data at the same ξ but higher (W^2, Q^2) from Ref. [59], shown here at $Q^2 = 5$ GeV^2.

W. Melnitchouk, R. Ent, and C. Keppel, Phys. Rept. 406 (2005) 127-301

Motivation for investigating Quark-Hadron duality

G. Domokos, S. Kovesi-Domokos, and E. Schonberg, Phys. Rev. D **3** (1971) 1184.

- This paper served as an early attempt to a scaling structure function built up from an "oscillator-like" resonance spectrum of n resonances, depending only on x_B.

Motivation for investigating Quark-Hadron duality

G. Domokos, S. Kovesi-Domokos, and E. Schonberg, Phys. Rev. D **3** (1971) 1184.

- This paper served as an early attempt to a scaling structure function built up from an "oscillator-like" resonance spectrum of n resonances, depending only on x_B.
- Revisiting this calculation is useful to bring the notation up to date and to discover exactly what properties of the resonance model lead to a scale-independent structure function.

Structure Functions

The structure functions W_1 and W_2 are defined in terms of the hadronic tensor $W_{\mu\nu}$.

$$W_{\mu\nu} = \left(-g_{\mu\nu} - \frac{q_\mu q_\nu}{q^2}\right) W_1 + \frac{1}{m^2}\left(p_\mu - \frac{p \cdot q}{q^2} q_\mu\right)\left(p_\nu - \frac{p \cdot q}{q^2} q_\nu\right) W_2$$

where p and q are the four-momenta of the incoming hadron and virtual photon, respectively.

Structure Functions

The structure functions W_1 and W_2 are defined in terms of the hadronic tensor $W_{\mu\nu}$.

$$W_{\mu\nu} = \left(-g_{\mu\nu} - \frac{q_\mu q_\nu}{q^2}\right) W_1 + \frac{1}{m^2}\left(p_\mu - \frac{p\cdot q}{q^2} q_\mu\right)\left(p_\nu - \frac{p\cdot q}{q^2} q_\nu\right) W_2$$

where p and q are the four-momenta of the incoming hadron and virtual photon, respectively.

The structure functions obtained in the paper by Domokos *et al.* were also obtained in an earlier paper by Bjorken and Walecka. The two papers use different methods of derivation to achieve the same result.

J. D. Bjorken and J. D. Walecka, Annals of Physics **38**, 35-62 (1966)

Structure Functions

$$W_1^{JnN} = \frac{M_n^5 |\vec{q}|^{2J+1}(E+m)P_N^2}{2^{J+3/2}m^2}\frac{(2J+1)!!}{(2J)!!}\left(\frac{2J+3}{2J-1}G_2^2 + G_3^2\right),$$

$$W_2^{JnN} = \frac{m^2Q^2}{M_n^2|\vec{q}|^2}W_1^{JnN} + \frac{M_n|\vec{q}|^{2J-1}(E+m)P_N^2}{2^{J+3/2}}\frac{(2J+1)!!}{(2J)!!}G_1^2,$$

where m is the initial nucleon mass, M_n is the mass of the resonance, $|\vec{q}|$ is the CM frame momentum of the two incoming particles, $Q^2 = -q^2$ is the virtuality of the incoming photon, E is the CM frame energy of the incoming nucleon, J is the final spin of the excited state nucleon, G_i is an invariant form factor, and P_N is a parity-dependent factor equivalent to

$$P_N = \begin{cases} 1, & N = 1 \\ \frac{|\vec{q}|}{E+m}, & N = -1 \end{cases}.$$

Elastic Case

$$W_1^{1/2,0,N} = \frac{m^3|\vec{q}|^2(E+m)P_N^2}{2} G_3^2 \delta\left(\nu - \frac{Q^2}{2m}\right),$$

$$W_2^{1/2,0,N} = \left(\frac{Q^2}{|\vec{q}|^2} W_1^{1/2,0,N} + \frac{m(E+m)P_N^2}{2} G_1^2\right) \delta\left(\nu - \frac{Q^2}{2m}\right).$$

(The $2m\delta\left((p+q)^2 - M_n^2\right) = \delta\left(\nu - \frac{Q^2}{2m}\right)$ factors were omitted from the previous slide for brevity)

Elastic Case

$$W_1^{1/2,0,N} = \frac{m^3|\vec{q}|^2(E+m)P_N^2}{2} G_3^2 \delta\left(\nu - \frac{Q^2}{2m}\right),$$
$$W_2^{1/2,0,N} = \left(\frac{Q^2}{|\vec{q}|^2} W_1^{1/2,0,N} + \frac{m(E+m)P_N^2}{2} G_1^2\right) \delta\left(\nu - \frac{Q^2}{2m}\right).$$

(The $2m\delta\left((p+q)^2 - M_n^2\right) = \delta\left(\nu - \frac{Q^2}{2m}\right)$ factors were omitted from the previous slide for brevity)

By defining $\tau = \frac{Q^2}{4m^2}$, the structure functions can be simplified to

$$W_1^{1/2,0,N} = 4m^6\tau(1+\tau)^2 P_N^2 G_3^2 \delta\left(\nu - \frac{Q^2}{2m}\right)$$
$$W_2^{1/2,0,N} = \left(\frac{W_1^{1/2,0,N}}{1+\tau} + m^2(1+\tau)P_N^2 G_1^2\right) \delta\left(\nu - \frac{Q^2}{2m}\right)$$

Elastic Case

By relating the previous structure function expressions to known ones,

$$W_1^{1/2,0,N} = \tau G_M^2 \delta\left(\nu - \frac{Q^2}{2m}\right),$$
$$W_2^{1/2,0,N} = \frac{G_E^2 + \tau G_M^2}{1+\tau} \delta\left(\nu - \frac{Q^2}{2m}\right),$$

we find that the elastic electric and magnetic form factors are related to G_1 and G_3 by

$$G_M = 2m^3(1+\tau)P_N G_3,$$
$$G_E = m(1+\tau)P_N G_1.$$

Form Factors in the Bjorken Limit

The full structure function W_1 is given by

$$\begin{aligned} W_1 &= \sum_{JnN} W_1^{JnN} = Ef(\Pi + \Delta), \\ &\to mEf(\mu_{1/2}^2 + \mu_{3/2}^2) \int_0^\infty \frac{B_n}{M_n} \left(1 + \frac{Q^2(mr)^2}{M_n^2}\right)^{-4} dn, \end{aligned}$$

where f is a free parameter, Π and Δ are the isospin $\frac{1}{2}$ and $\frac{3}{2}$ contributions, respectively, μ_I is the magnetic moment of the nucleon with isospin I, r is the effective radius of the nucleus, and B_n is a Breit-Wigner factor.

Form Factors in the Bjorken Limit

The full structure function W_1 is given by

$$\begin{aligned} W_1 &= \sum_{JnN} W_1^{JnN} = Ef(\Pi + \Delta), \\ &\to mEf(\mu_{1/2}^2 + \mu_{3/2}^2) \int_0^\infty \frac{B_n}{M_n} \left(1 + \frac{Q^2(mr)^2}{M_n^2}\right)^{-4} dn, \end{aligned}$$

where f is a free parameter, Π and Δ are the isospin $\frac{1}{2}$ and $\frac{3}{2}$ contributions, respectively, μ_I is the magnetic moment of the nucleon with isospin I, r is the effective radius of the nucleus, and B_n is a Breit-Wigner factor.
From here, the limit as $Q^2 \to \infty$ is taken and the variable $\omega' = \frac{2p\cdot q + m^2}{Q^2}$ is defined, which is equivalent to $\frac{1}{x_B}$ in the high Q^2 limit.

Form Factors in the Bjorken Limit

Finally, we can make a change of variables to $u = \frac{M_n^2}{m^2 Q^2}$ with $dn = Q^2 du$ so that

$$W_1 \approx \frac{\omega' f}{2\sqrt{\omega' - 1}} (\mu_{1/2}^2 + \mu_{3/2}^2) \int_0^\infty \frac{1}{\sqrt{u}} Q^2 B_n \left(1 + \frac{r^2}{u}\right)^{-4} du.$$

Form Factors in the Bjorken Limit

Finally, we can make a change of variables to $u = \frac{M_n^2}{m^2 Q^2}$ with $dn = Q^2 du$ so that

$$W_1 \approx \frac{\omega' f}{2\sqrt{\omega' - 1}} (\mu_{1/2}^2 + \mu_{3/2}^2) \int_0^\infty \frac{1}{\sqrt{u}} Q^2 B_n \left(1 + \frac{r^2}{u}\right)^{-4} du.$$

The other structure function $F_2 = \nu W_2$ has similar properties, as it is proportional to W_1 in the high Q^2 limit. The final result of Domokos *et al.* is that

$$F_2 \approx f(\mu_{1/2}^2 + \mu_{3/2}^2) \frac{(\omega' - 1)^3}{(\omega' - 1 + m^2 r^2)^4}.$$

when B_n is replaced with a delta function.

Breit-Wigner factor

The Breit-Wigner factor is used to replace the delta function

$$\delta\left(s - M_n^2\right) \to B_n = \frac{1}{\pi} \frac{\Gamma_0 M_n^2}{(s - M_n^2)^2 + (\Gamma_0 M_n^2)^2},$$

where Γ_0 is some initial resonance width and $s = (p+q)^2$.

Breit-Wigner factor

The Breit-Wigner factor is used to replace the delta function

$$\delta\left(s - M_n^2\right) \to B_n = \frac{1}{\pi}\frac{\Gamma_0 M_n^2}{(s - M_n^2)^2 + (\Gamma_0 M_n^2)^2},$$

where Γ_0 is some initial resonance width and $s = (p+q)^2$. When converting to the variable u and taking the high Q^2 limit, this becomes

$$B_n \quad = \frac{1}{\pi Q^2}\frac{\Gamma_0 m^2 u}{(\omega' - 1 - m^2 u)^2 + (\Gamma_0 m^2 u)^2}$$

so that $Q^2 B_n$ becomes independent of Q^2. In fact, any function in place of B_n that goes with $\frac{1}{M_n^2}$ in the high Q^2 limit will have this property.

Summary

- The structure functions given in Domokos *et al.* were updated to modern language. Their relation to the elastic electric and magnetic form factors was established.

Summary

- The structure functions given in Domokos *et al.* were updated to modern language. Their relation to the elastic electric and magnetic form factors was established.
- The $\frac{1}{M_n^2}$ dependence of the Breit-Wigner factor B_n was shown to be important in making the structure functions scale independent at high Q^2.

Summary

- The structure functions given in Domokos *et al.* were updated to modern language. Their relation to the elastic electric and magnetic form factors was established.
- The $\frac{1}{M_n^2}$ dependence of the Breit-Wigner factor B_n was shown to be important in making the structure functions scale independent at high Q^2.
- More research into the scale independence is to be done.

Motivation for New Project

- From a paper by Jen-Chieh Peng *et al.* (arXiv:1401.1705)

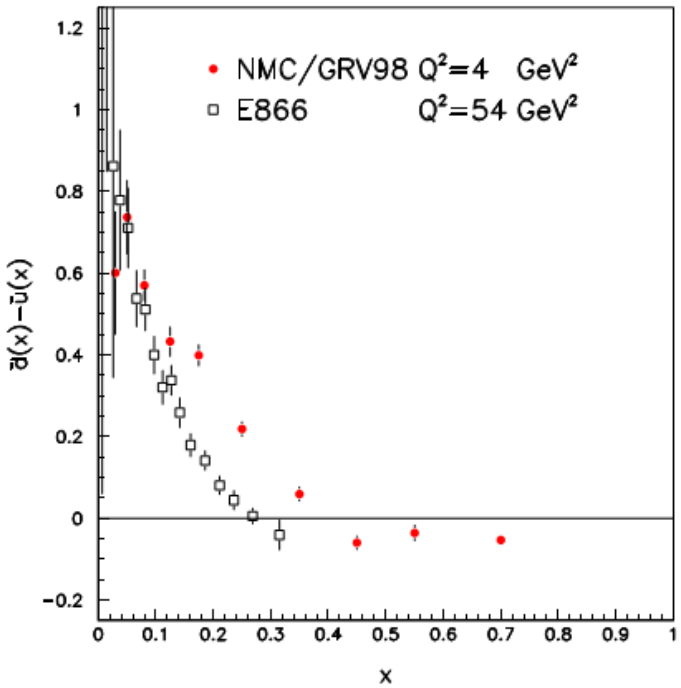

FIG. 2: Values of $\bar{d}(x) - \bar{u}(x)$ at $Q^2 = 4$ GeV^2 evaluated using Eq. (2), as discussed in the text. Also shown are the values of $\bar{d}(x) - \bar{u}(x)$ at $Q^2 = 54$ GeV^2 from the Fermilab E866 experiment.

Motivation for New Project

- From a paper by Jen-Chieh Peng *et al.* (arXiv:1401.1705)
- Want to investigate apparent discrepancy in the data sets.

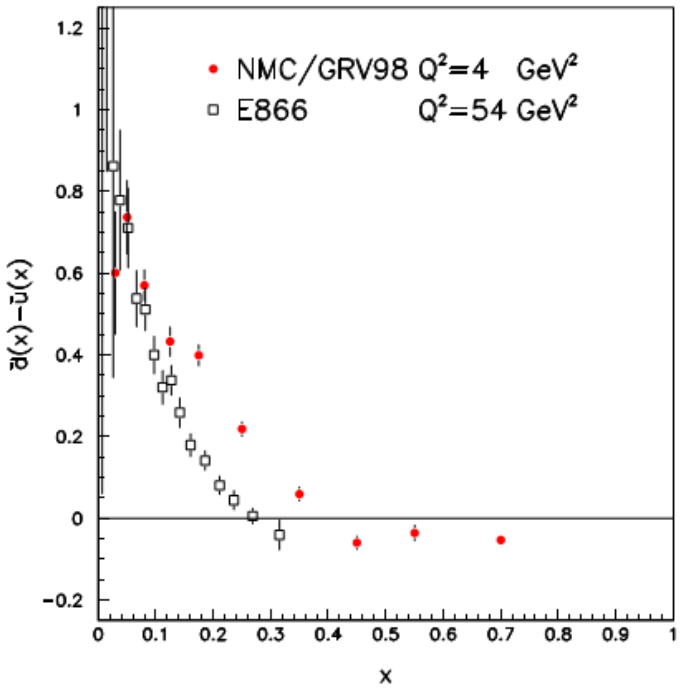

FIG. 2: Values of $\bar{d}(x) - \bar{u}(x)$ at $Q^2 = 4$ GeV^2 evaluated using Eq. (2), as discussed in the text. Also shown are the values of $\bar{d}(x) - \bar{u}(x)$ at $Q^2 = 54$ GeV^2 from the Fermilab E866 experiment.

Motivation for New Project

- From a paper by Jen-Chieh Peng *et al.* (arXiv:1401.1705)
- Want to investigate apparent discrepancy in the data sets.
- Identified two problems with how the NMC data are used here

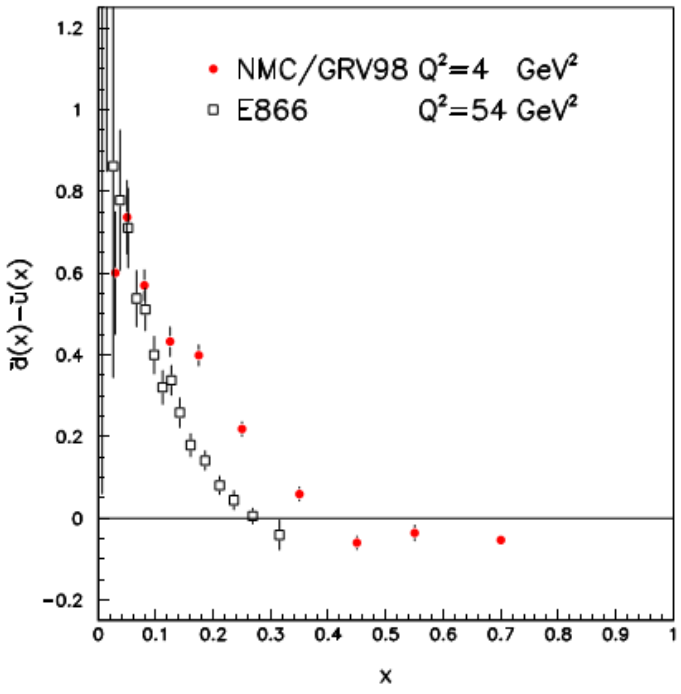

FIG. 2: Values of $\bar{d}(x) - \bar{u}(x)$ at $Q^2 = 4$ GeV^2 evaluated using Eq. (2), as discussed in the text. Also shown are the values of $\bar{d}(x) - \bar{u}(x)$ at $Q^2 = 54$ GeV^2 from the Fermilab E866 experiment.

$\bar{d} - \bar{u}$ plots and comparisons

In particular, the paper used the leading order relation

$$F_2^p(x) - F_2^n(x) = \frac{x}{3}\left(u(x) + \bar{u}(x) - d(x) - \bar{d}(x)\right)$$

to derive

$$\begin{aligned}\bar{d}(x) - \bar{u}(x) &= u(x) - d(x) - \frac{3}{x}\left(F_2^p(x) - F_2^n(x)\right) \\ &= \frac{1}{2}\left(u_v(x) - d_v(x) - \frac{3}{x}\left(F_2^p(x) - F_2^n(x)\right)\right)\end{aligned}$$

$\bar{d} - \bar{u}$ plots and comparisons

In particular, the paper used the leading order relation

$$F_2^p(x) - F_2^n(x) = \frac{x}{3}\left(u(x) + \bar{u}(x) - d(x) - \bar{d}(x)\right)$$

to derive

$$\begin{aligned}\bar{d}(x) - \bar{u}(x) &= u(x) - d(x) - \frac{3}{x}\left(F_2^p(x) - F_2^n(x)\right) \\ &= \frac{1}{2}\left(u_v(x) - d_v(x) - \frac{3}{x}\left(F_2^p(x) - F_2^n(x)\right)\right)\end{aligned}$$

Also want to look at the effects of nuclear smearing and off-shell corrections.

$\bar{d} - \bar{u}$ plots and comparisons

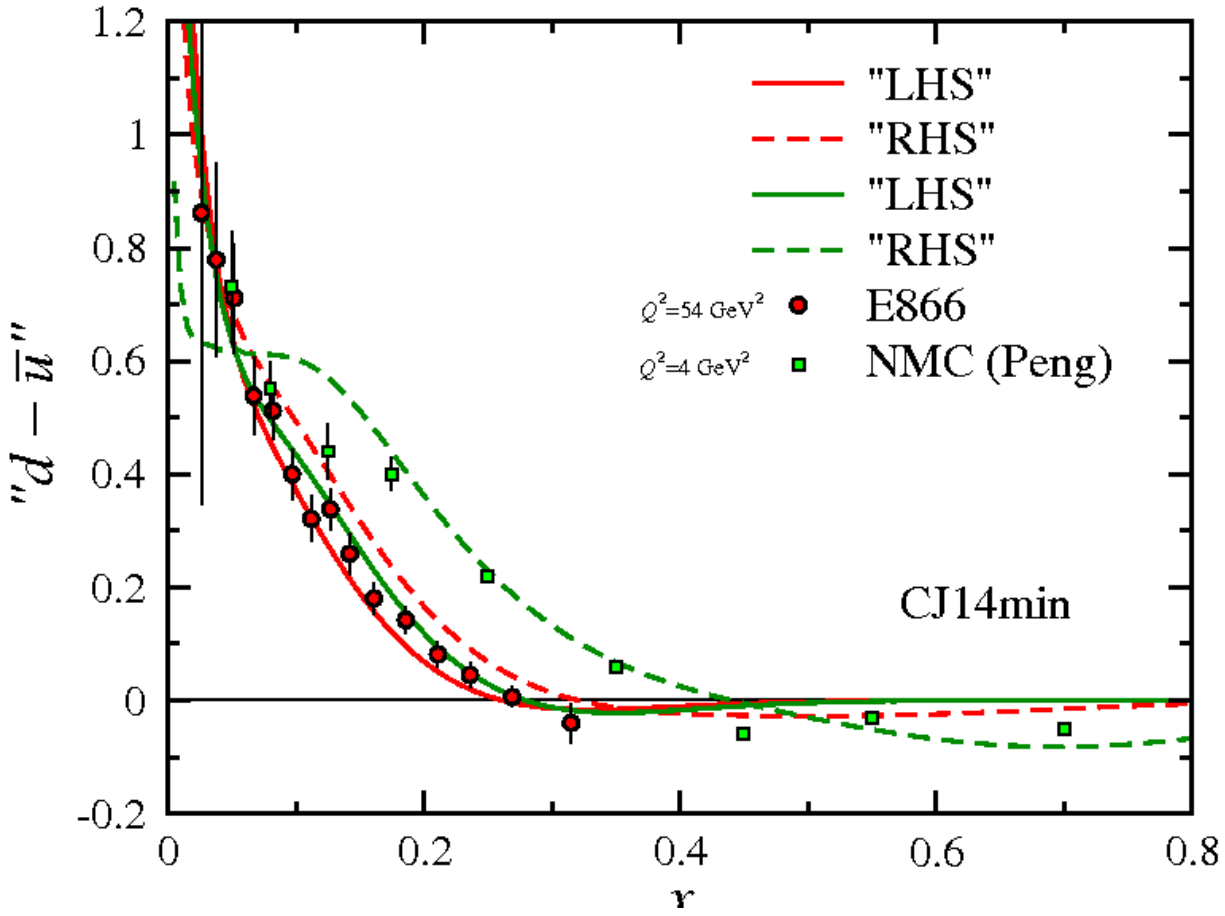

$\bar{d} - \bar{u}$ plot errors

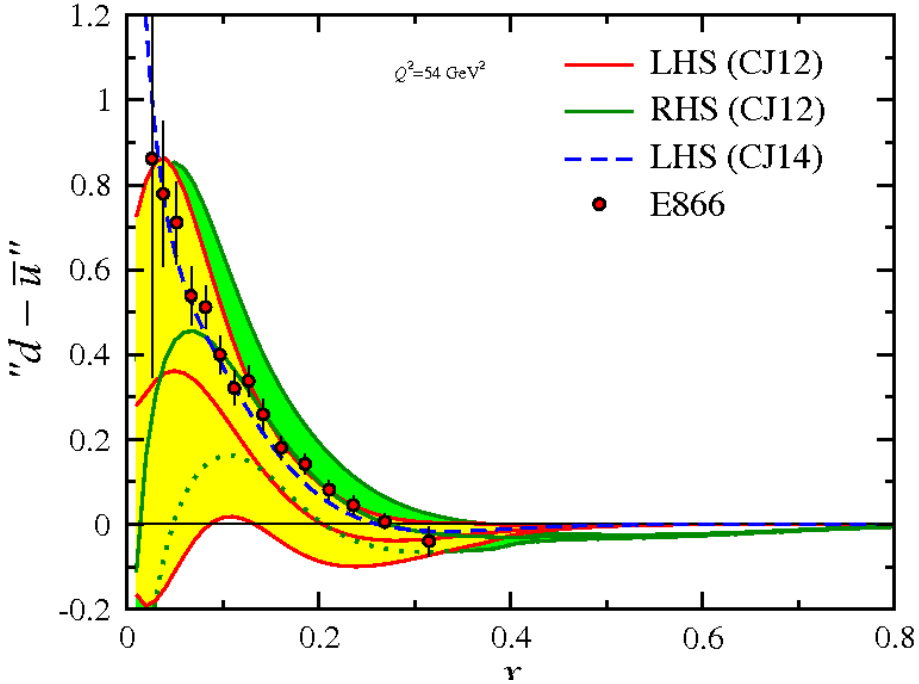

Also calculated these relations with errors using CJ12 PDF grids, as detailed in Owens *et al.* (Sec. II E, Phys. Rev. D 87, 094012 (2013)).

DY addition to CJ code

Also added a routine to the CJ14 fitting package to compute nuclear smearing and off-shell corrections for the Drell-Yan deuteron cross-section.

The corrections come from Ehlers *et al.* At the GeV scale, the smearing is approximately the same as that of DIS at $\gamma = 1$, and the fmKP off-shell model is valid for both DIS and Drell-Yan.

P. J. Ehlers, A. Accardi, L. Brady, and W. Melnitchouk, Phys. Rev D **90**, 014010 (2014)

DY addition to CJ code

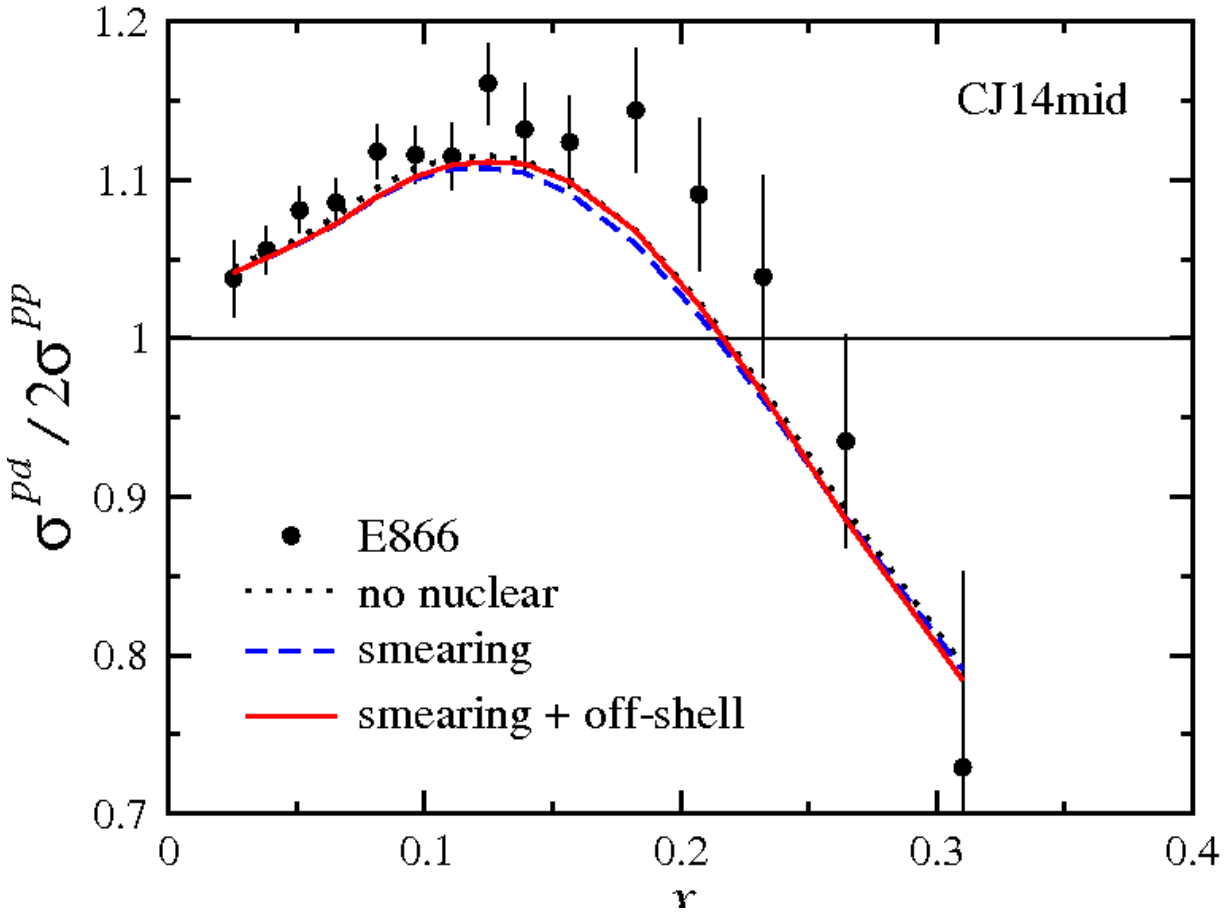

Summary

- The amount by which the LO equation $F_2^p(x) - F_2^n(x) = \frac{x}{3}\left(u(x) + \bar{u}(x) - d(x) - \bar{d}(x)\right)$ fails to hold at NLO was quantified.

Summary

- The amount by which the LO equation $F_2^p(x) - F_2^n(x) = \frac{x}{3}\left(u(x) + \bar{u}(x) - d(x) - \bar{d}(x)\right)$ fails to hold at NLO was quantified.
- Error calculations on the above equation solved for $\bar{d} - \bar{u}$ were performed.

Summary

- The amount by which the LO equation $F_2^p(x) - F_2^n(x) = \frac{x}{3}\left(u(x) + \bar{u}(x) - d(x) - \bar{d}(x)\right)$ fails to hold at NLO was quantified.
- Error calculations on the above equation solved for $\bar{d} - \bar{u}$ were performed.
- Drell-Yan smearing and off-shell routines were added into the CJ14 fitting package.

Summary

- The amount by which the LO equation $F_2^p(x) - F_2^n(x) = \frac{x}{3}\left(u(x) + \bar{u}(x) - d(x) - \bar{d}(x)\right)$ fails to hold at NLO was quantified.
- Error calculations on the above equation solved for $\bar{d} - \bar{u}$ were performed.
- Drell-Yan smearing and off-shell routines were added into the CJ14 fitting package.
- Various other theoretical calculations were performed using CJ14.